A MACROMECHANICAL CONSTITUTIVE MODEL OF SHAPE MEMORY ALLOYS UNDER UNIAXIAL CYCLIC LOADING

H. Lei * **B. Zhou** **Z. Wang** **Y. Wang**

College of Aerospace and Civil Engineering
Harbin Engineering University
Harbin 150001, China

ABSTRACT

In this paper, the thermomechanical behavior of shape memory alloys (SMAs) subjected to uniaxial cyclic loading is investigated. To obtain experimental data, the strain-controlled cyclic loading-unloading tests are conducted at various strain-rates and temperatures. Dislocations slip and deformation twins are considered to be the main reason that causes the unique cyclic mechanical behavior of SMAs. A new variable of shape memory residual factor was introduced, which will tend to zero with the increasing of the number of cycles. Exponential form equations are established to describe the evolution of shape memory residual factor, elastic modulus and critical stress, in which the influence of strain-rate, number of cycles and temperature are taken into account. The relationship between critical stresses and temperature is modified by considering the cycling effect. A macromechanical constitutive model was constructed to predict the cyclic mechanical behavior at constant temperature. Based on the material parameters obtained from test results, the hysteretic behavior of SMAs subjected to isothermal uniaxial cyclic loading is simulated. It is shown that the numerical results of the modified model match well with the test results.

Keywords: Superelastic, Cyclic loading, Residual strain.

1. INTRODUCTION

Shape memory alloys (SMAs) are a class of metals that exhibit several extraordinary properties, for instance the shape memory effect (SME), excellent physical chemical character, superelasticity (SE), and high damping capacity. Due to these special performances, SMAs have been widely used as major elements in civil engineering structures, aircraft structures and so on. However, these elements are usually subjected to various cyclic loadings. Increasing number of cycles, phase transformation behavior and mechanical properties of SMAs will change gradually. Therefore, it is necessary to develop a reasonable model to predict the mechanical behaviors of SMAs under cyclic loading.

In the previous studies, many constitutive models have been established to describe the SE and SME of ideal shape memory alloy [1-6]. Brinson [1] developed a one-dimensional constitutive model based on previous studies. An internal variable was used to derive a comprehensive constitutive law for shape memory alloy materials from first principles without the assumption of constant material functions. Zhou *et al.* [6] defined a new concept, shape memory factor, and he developed a new phase transition equation, which truly expresses the influence of phase transformation peak temperature and describes the transformation from twinned martensite to detwinned martensite. However， these models are not suitable for predicting the cyclic behavior of SMAs due to the complexity of micro-to-macro transition.

According to experimental observations, the stress-strain superelastic loop of SMA is not closed. A permanent inelastic strain remains, which is accumulated with the number of cycles. The particular behavior is defined as “ratcheting effect” by Feng and Sun [7]. In present, some mechanical models are constructed to describe the particular behavior by introducing internal variables in the framework of generalized plasticity, based on strain-controlled or stress-controlled cyclic tensile-unloading tests [8-15]. Lubliner *et al.* [8] first attempted to apply generalized plasticity to describe the thermomechanical behavior of shape memory alloys, and they developed an one-dimensional model based on a local rate-independent internal variable (stress-induced accumulation of martensite fraction). Gong *et al.* [9] introduced three internal variables, namely residual stress, residual strain and residual martensite, to characterize the cyclic superelastic deformation. The elastic modulus during the internal loop was expressed by a mixed rule with the function of transformation strain. Mal´ecot *et al.* [10] introduced residual stress, residual strain and volume fraction of the residual

* Corresponding author (lei123shuai@126.com)

DOI : 10.1017/jmech.2012.56
Copyright © 2012 The Society of Theoretical and Applied Mechanics, R.O.C.
https://doi.org/10.1017/jmech.2012.56 Published online by Cambridge University Press

martensite accumulated during the cycling, and they modeled the cyclic thermal dissipation based on the thermo-equilibrium equation. Zaki and Moumni [11] developed a three-dimensional model to describe the behaviors of SMAs under cyclic loading by introducing three state variables: Internal stress, residual strain and cumulated martensite volume fraction. Luc *et al.* [12] and Auricchio *et al.* [13] developed a three-dimensional model to describe the evolution of permanent inelastic strain under cyclic loading respectively, based on a series of tensile tests. Kan and Kang [14,15] investigated the uniaxial transformation ratcheting of superelastic SMAs at room temperature, and they constructed a new phenomenological constitutive model, in which the effect of cycles was taken into account, by introducing a new internal variable (cumulated martensite volume fraction) under the consideration of the incompletely reverse thermoelastic martensitic phase transformation and transformation-induced plastic strain. By summarizing the different approaches discussed above, it can be found that various internal variables were introduced to describe the evolution of permanent inelastic strain. The mathematic expressions are complicated. Therefore the application in structural engineering is limited.

Recently, many reasons for the origin of residual strain during superelastic cycling are presented. In general, these reasons can be divided into three types as follows: (1) the cyclic accumulation of stress-induced residual martensite causes the increase of residual deformation; (2) the cyclic accumulation of transformation-induced plastic strain causes the increase of irreversible strain; (3) the cyclic accumulation of temperature-induced and stress-induced dislocation slip causes the increase of permanent deformation. In a recent literature, Delville *et al.* [16] investigated the dislocation slip during superelastic cycling of Ni-Ti wires, and the transmission electron microscopy observation illustrated that none or very little residual martensite phase was found in the microstructures of superelastically cycled wires. Thus, dislocations slip and deformation twins were considered as the major affective factors that caused the unique hysteretic behavior of SMAs.

In addition, Ren [17] investigated the hysteretic responses of superelastic SMAs subjected to cyclic isothermal simple tension loading, and they established a modified multi-linear constitutive model in the framework of general thermodynamic developed by Lagoudas [18]. The relationship between critical stresses and austenite elastic modulus, and cycle number was considered as an approximately linear function. The model was simple and easy-to-use in engineering. However, the simulation results were inconsistent with the experiment result presented in their paper.

In this paper, a macromechanical constitutive model was constructed to predict the cyclic mechanical behavior at constant temperature based on a series of uniaxial strain-controlled cyclic tensile tests and differential scanning colorimeter (DSC) tests of superelastic Ni- Ti SMA wires. Dislocations slip and deformation twins were considered as the main reason which caused the unique cyclic mechanical behavior of SMA. A new variable of shape memory residual factor was introduced, which tends to zero with the increasing of number of cycles. Exponential form equations were established to describe the evolution of shape memory residual factor, elastic modulus and critical stress, respectively. Based on the material parameters obtained from test results, simulations were carried out to make comparisons with the experimental results based on the proposed model. Comparing the corresponding experimental results and simulation results, it was demonstrated the validity of the present constitutive model to predict the cyclic mechanical behavior of SMA.

2. EXPERIMENTS

2.1 Uniaxial Cyclic Loading-Unloading Tests

The test specimens used are superelastic Ni-Ti (50%) SMA wires with a diameter of 1mm, length of 150mm, and calibration length of 100mm. A sketch of the experimental set-up is shown in Fig. 1. The test specimen is heated electrically, and the steady current is controlled by a DC power supply. The surface temperature of the specimen was measured by a thermocouple, and then feed back to the host controller. In a typical test, one end of the wire is connected to the fixed platform and the other end was fixed to the movable beam. Stress and strain signals are transferred to the host controller (data acquisition system) with a sampling rate of 10 samples per second. In this article, a universal testing machine (Instron4505) was used to conduct the loading tests.

As the main objective of this paper is to investigate the behavior during the cycles, a series of tests at various strain-rates ($\dot{\varepsilon}$ = 1%/min, 3%/min, 5%/min, and 7%/min) were performed up to 20 cycles, under a constant temperature (343K, above austenite finish temperature). Considering the influence of strain on the phase transformation, the maximum strain of 12% was selected in this test to ensure a complete austenite-martensite transformation.

The typical stress-strain curves are shown in Fig. 2. For further investigation of the cyclic properties, we redefined the concept of residual strain ε_r which is irrecoverable in each complete loading-unloading loop, and ε_{ri} was the residual strain of the ith cycle. Some general phenomenon can be observed during the test. The residual strain decreases with cycle number and will disappear when the cycle number is sufficiently large, the material gradually tends to be an approximately stable superelastic state. In practice SMAs are often loaded and unloaded repeatedly to obtain a stable superelastic behavior, which is usually called "training process".

As we known, the dissipated energy is produced by releasing of heat energy during the phase transformation from austenite to martensite and the reverse transformation back to austenite. According to Fig. 2, the phase transformation critical stresses changes with the number of cycles, and the dissipated energy (as shown in Fig. 3) has an obvious decreasing tendency in the

https://doi.org/10.1017/jmech.2012.56 Published online by Cambridge University Press

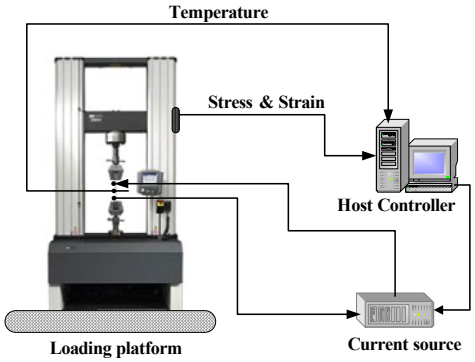


Fig. 1 Sketch of the experimental set-up

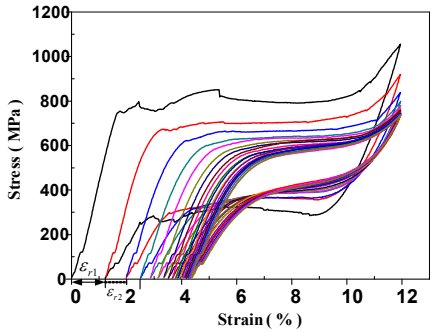


Fig. 2 Typical stress-strain curves (N = 20, $\dot{\varepsilon}$ = 7%/min)

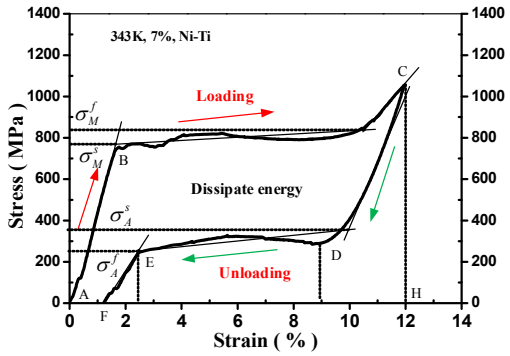


Fig. 3 Illustration of dissipated energy of Ni-Ti during first cycle

initial several cycles, then the tendency becomes gentle in the following cycles. Figure 3 represents a typical experiment results, which shows a complete loop (loading and unloading) of a sample in tensile. In this figure, the area of S_{ABCDEF} is the dissipated energy. σ^s_M and σ^f_M denote the austenite to martensite transformation start and finish stress, defined by the intersection of the lines that are tangent to the initial elastic and the upper plateau of the loading stress–strain curve. σ^s_A and σ^f_A denote the martensite to austenite transformation start and finish stress.

2.2 Differential Scanning Colorimeter (DSC) Tests

In addition, a series of DSC tests is conducted to investigate the phase transformation behaviors of Ni-Ti (50%) wire. The temperature scanning range is from 223K to 393K. During the experiment, samples are heated to 393K, held there for 1min, and cooled to 223K at the rate of 5K/min. Then samples held there for 1min and heated again to 393K at the same rate of 5K/min.

Figure 4 shows the heat flow–temperature curves for determining the phase transformation temperatures of shape memory alloy. A_s, A_f, M_s and M_f are the austenite starting temperature, austenite finishing temperature, martensite starting temperature and martensite finishing temperature, respectively. A_p and M_p are the phase transformation peak temperatures [6], which as well as phase transformation starting and finishing temperatures are the main factors affecting the phase transformation behaviors of SMA.

3. SHAPE MEMORY RESIDUAL FACTOR

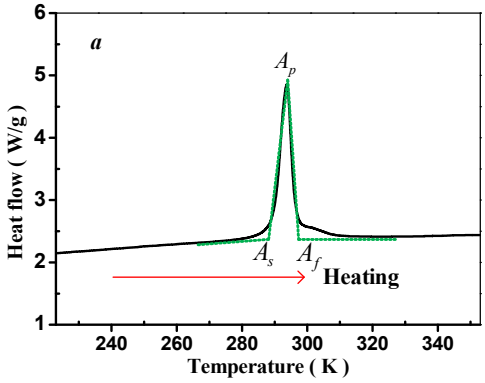
In order to characterize the effect of dislocation slip and deformation twins on the mechanical behavior of shape memory alloy, a new variable of shape memory residual factor η_r was introduced based on the ref. [6]. It is expressed as follows

$$\eta_{ri} = \frac{\varepsilon_{ri}}{\varepsilon_L} \tag{1}$$

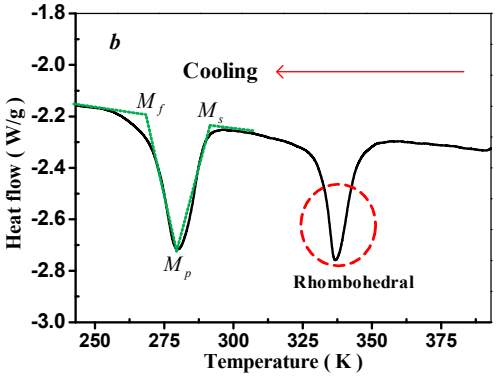
where ε_L is the maximum shape memory strain, a material constant of SMA. It can be determined through tensile test at the temperature below austenite starting temperature. In this equation, a macroscopic parameter is employed to describe the change of two microscopic factors. Due to the presence of shape memory residual factor, the shape memory process of SMA can be modified as shown in Fig. 5.

Figure 5 shows the evolution of shape memory residual factor during one loading-unloading cycle. At the beginning of loading, the material remains to be a pure austenite phase; therefore the value of shape memory factor is zero. When $\sigma > \sigma^s_M$, the material will transform from austenite to martensite gradually, and the shape memory factor will increase from 0 to 1 with the increase of applied stress. During the process of unloading, the material remains to be fully martensite phase before the stress less than the austenite start stress (σ^s_A). Then, the material will gradually transform from martensite to austenite, and shape memory effect will dominant the deformation. When $\sigma < \sigma^f_A$, due to the generation of dislocation slip and deformation twins, a residual strain remains after unloading and the value of shape memory factor cannot completely vanish. The part indicated in the red circle represents the value of shape memory residual factor proposed in this article. With the increasing of cycle number, the value of η_r tends to zero, it indicates that the SME and SE are gradually strengthened. In the next cycle, we assume that the shape memory residual factor is not accumulated during cycling.

https://doi.org/10.1017/jmech.2012.56 Published online by Cambridge University Press



(a) Heating



(b) Cooling

Fig. 4 Heat flow-temperature curve of DSC test

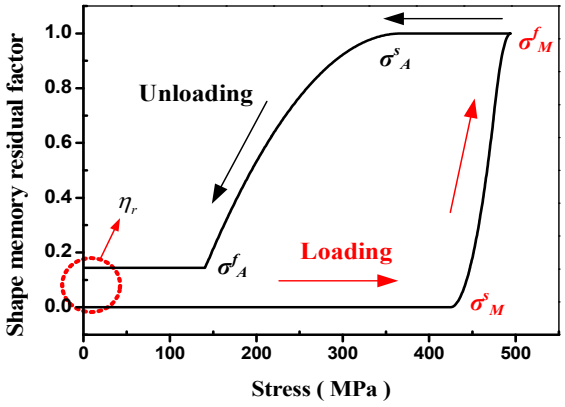


Fig. 5 Evolution of shape memory residual factor during one cycle

4. EVOLUTION EQUATION OF SHAPE MEMORY RESIDUAL FACTOR

In the previous literature, Tobushi [19], Nemat-Nasser [20,21] and Lee [22] investigated the influence of strain-rate and temperature on the deformation of SMAs, and they investigated the strain-rate sensitivity of the transition stress for stress-induced martensite transformation. In this work, constant strain amplitude is applied to the superelastic Ni-Ti alloy at various temperatures and strain-rates; therefore the effect of strain amplitude is neglected. The residual strain is measured by uniaxial tensile tests at various temperatures and strain-rates respectively.

Figure 6 shows the curves of residual strain ($i = 1$) at different temperatures (above austenite finish temperature) and strain-rates. It can be seen from the experimental results that the residual strain increases almost linearly with the temperature and the strain-rate. Based on previous study [23], we assume that the residual strain only depends on the number of cycles, strain-rate and temperature in this paper.

Based on Eq. (1), the evolution equation of shape memory residual factor is expressed as follows:

$$\eta_{ri}(i,T,\dot{\varepsilon}) = \frac{1}{\varepsilon_L}\left(a\dot{\varepsilon} + b(T-T_0) + c\right)\exp\left(-\beta\,(i-1)\right) \qquad (2)$$

in which a is a strain-rate-dependent constant, b is a temperature-dependent constant, c represents the material constant, and β is a cycle-dependent parameter, which controls the evolution rate of shape memory residual factor. T_0 is the initial value of temperature. These parameters will be determined from the experimental results.

According to Eq. (2), the variation tendency of shape memory residual factor with different conditions (number of cycles, strain-rate and temperature) can be predicted. Figure 7 shows the comparison of experimental results and theoretical results according to Eq. (2) under the condition of different strain-rates (3%/min and 7%/min) and constant temperature (343K). It can be seen from the figure that the residual strain decrease rapidly with the number of cycles at the first several cycles, while it will tend to be zero when the cycle number is large enough. The theoretical results agree well with the experimental results at both the specified strain-rates, which illustrates the precision and rationality of evolution equation given in present paper.

5. EVOLUTION EQUATION OF ELASTIC MODULUS

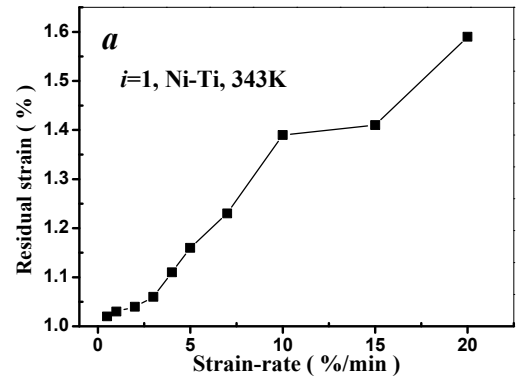
Generally, the elastic modulus of material will change slightly due to the effect of cycle. As shown in Fig. 2, the slopes of stress-strain curves before and after transformation decrease with the increasing of the number of cycles, however the decreasing amplitude gradually reduces. Eventually, the value of slope tends to be a constant. For simplicity, the same changing trends of the elastic modulus of martensite and austenite during cycling are assumed.

An exponential equation was established based on the experimental results. The equation of elastic modulus is expressed as:

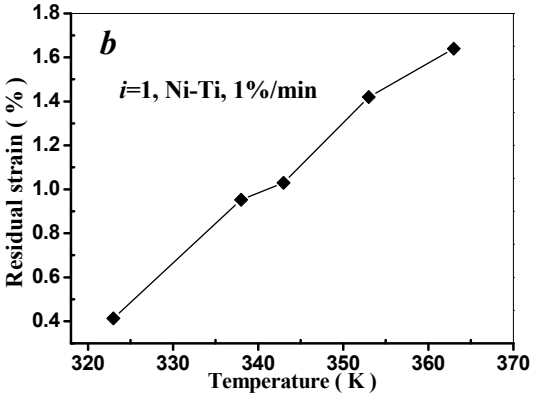
$$E'(i) = \left(E'(1) - \bar{E}\right)\exp\left(-\beta(i-1)\right) + \bar{E} \qquad (3)$$

where β is a cycle-dependent parameter, $E'(1)$ is the austenite and martensite elastic modules of the virgin SMA, $E'(1)$ is the modulus of the i^{th} cycle. $\bar{E}$ is the elastic modulus of the SMA which obtained a stable superelastic behavior by repeatedly training.

https://doi.org/10.1017/jmech.2012.56 Published online by Cambridge University Press

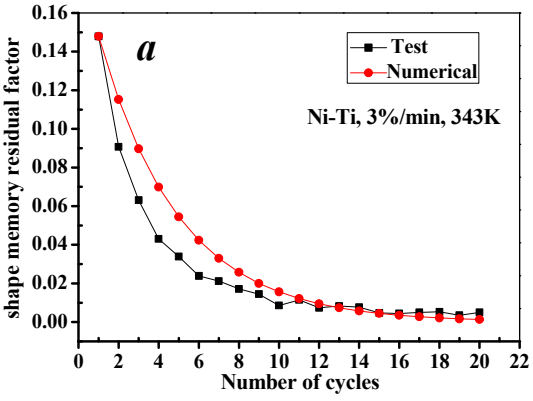


(a) Strain-rate

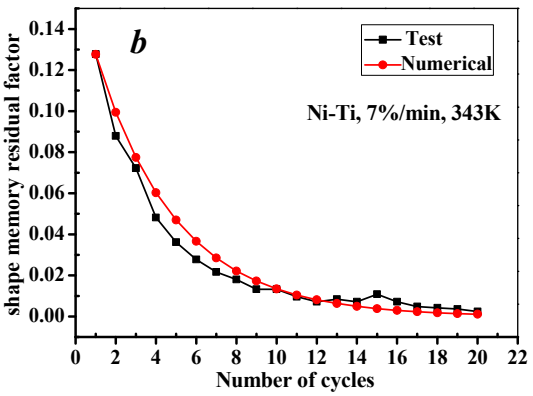


(b) Temperature

Fig. 6 The curves of residual strain (i = 1) at different



(a) 3%/min



(b) 7%/min

Fig. 7 Comparison of test and numerical results at different strain-rates (β = 0.25)

According to Eq. (3), the relationship of elastic modulus and cyclic number under isothermal cyclic tensile loading-unloading can be plotted as shown in Fig. 8, the experimental results and Ren's results are also presented for comparison. The line with rectangles, diamonds and triangles represents the results of experiment, Ren's method and the method presented in this paper respectively. By comparison, the theoretical result of the present method is in good agreement with the experimental result.

6. EVOLUTION EQUATIONS OF CRITICAL STRESSES

Critical stresses are important parameters, which describe the phase transformation behavior of SMA. Due to the effect of cycling, transformation critical stresses will gradually change and reach a saturated value eventually when the cycle number is large enough. However, a particular phenomenon different from previous literature was found based on the experimental results as shown in Fig. 9. It can be found from the stress-time curves that martensite critical stress gradually decreases, while the austenite critical stress slightly increases with increasing number of cycles.

In order to predict the process of critical stresses evolution from the initial values to their stable ones with the increasing of number of cycles, an exponential form evolution equation same as the form of elastic modulus is proposed based on the experimental results,

$$\sigma'_M(i) = \bar{\sigma}_M + \left(\sigma'_M(1) - \bar{\sigma}_M\right)\exp\left(-\psi_1(i-1)\right) \tag{4-1}$$

$$\sigma'_A(i) = \bar{\sigma}_A - \left(\bar{\sigma}_A - \sigma'_A(1)\right)\exp\left(-\psi_2(i-1)\right) \tag{4-2}$$

where σ'_M is the start and finish transformation stress of martensite, σ'_A is the start and finish transformation stress of austenite. The parameters ψ_1 and ψ_2 govern the saturated rates of the transformation stress during the cyclic phase transformation. For simplicity, we set $\psi_1 = \psi_2 = 0.25$.

As we known, Tanaka [24] and Brinson [1] employed two material parameters to describe the relationship of transformation critical stress and temperature, namely:

$$\sigma_M = C_M \Delta T \quad \sigma_A = C_A \Delta T \tag{5}$$

where σ_M and σ_A represent the critical stresses of martensite and austenite respectively. C_M and C_A are the stress influence coefficients, which are the slopes of the critical stress-temperature plots for the austenite and martensite transformation boundaries (the solid lines as shown in Fig. 10).

According to Eqs. (4) and (5), it can be found that the stress influence coefficients will change with the increasing number of cycles the expressions are given as follows

$$C'_M(i) = C'_M(1)\frac{\sigma'_M(i)}{\sigma'_M(1)} \quad C'_A(i) = C'_A(1)\frac{\sigma'_A(i)}{\sigma'_A(1)} \tag{6}$$

where $C'_M(i)$ and $C'_A(i)$ are the slopes in the i^{th} cycle.

https://doi.org/10.1017/jmech.2012.56 Published online by Cambridge University Press

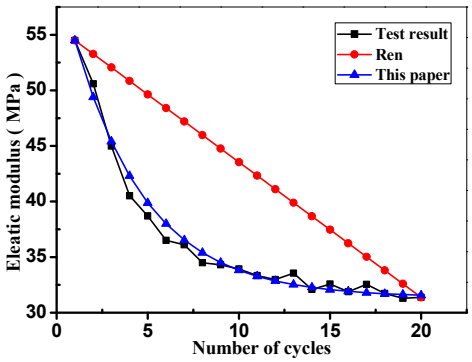


Fig. 8 Relationship of austenite elastic modulus and number of cycles (β = 0.25) (3%/min, 343K)

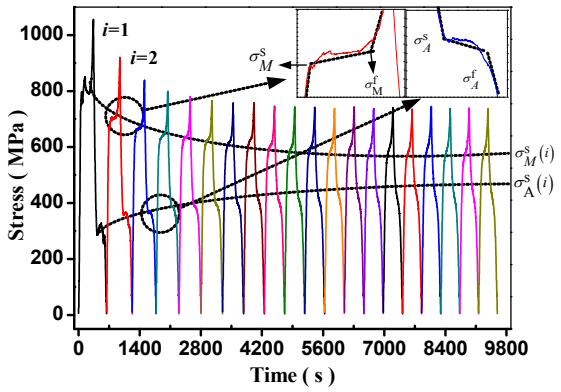


Fig. 9 The curves of stress-time (3%/min, 343K)

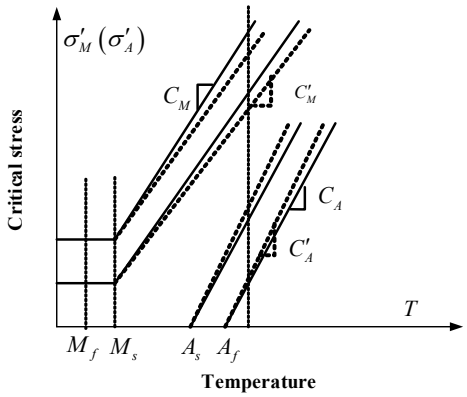


Fig. 10 Effect of cycling on the relationship between critical stress and temperature

According to the Eqs. (4) ~ (6), the relationship of phase transformation critical stresses and temperature can be modified. The modified critical stress-temperature plots are presented in Fig. 10, the dashed line represents the new relationship after cycles. It indicated the cycles have a significant influence on the slopes of the critical stress-temperature curves. At a constant temperature, the value of martensite critical stress gradually decreases with increasing of cycles, which causes reduction of the slope of critical stress-temperature curves as shown in Fig. 10. However, the value of austenite critical stresses slowly increases and the slopes of austenite critical stress-temperature curves increases with the number of cycles. It indicated that the effect of cycles on martensite is more significant than austenite.

7. PHASE TRANSFORMATION EQUATION

Another important problem is to construct a complete phase transformation equation to describe the phase transformation behavior of cycling. According to the definition of shape memory factor, an equation in which the influence of peak temperature is considered has been established. In this section, taking into account shape memory residual factor, the phase transformation equation [6] is further modified.

1. from austenite to martensite (η from 0 to 1):

$$\eta = s_1\left[\bar{\sigma} - \sigma_s^{cr} - C'_M(i)(T-M_s)_+^1\right]^2$$
$$\sigma_s^{cr} + C'_M(i)(T-M_s)_+^1 < \bar{\sigma} < \sigma_p^{cr} + C'_M(i)(T-M_s)_+^1 \quad (7\text{-}1)$$

$$\eta = s_2\left[\bar{\sigma} - \sigma_f^{cr} - C'_M(i)(T-M_s)_+^1\right]^2 + 1$$
$$\sigma_p^{cr} + C'_M(i)(T-M_s)_+^1 < \bar{\sigma} < \sigma_f^{cr} + C'_M(i)(T-M_s)_+^1 \quad (7\text{-}2)$$

where

$$(T-M_s)_+^1 = \begin{cases} T-M_s, & T > M_s \\ 0, & T \le M_s \end{cases}$$

2. from martensite to austenite (η from 1 to η_{ri}) ($T > A_s$):

$$\eta = \eta_u\left\{\frac{a_1}{C'_A(i)^2}\left[\bar{\sigma} - C'_A(i)(T-A_s)\right]^2 + 1\right\}$$
$$C'_A(i)(T-A_s) > \bar{\sigma} > C'_A(i)(T-A_p) \quad (7\text{-}3)$$

$$\eta = \eta_u\left\{\frac{a_2}{C'_A(i)^2}\left[\bar{\sigma} - C'_A(i)(T-A_f)\right]^2\right\}$$
$$C'_A(i)(T-A_p) > \bar{\sigma} > C'_A(i)\left(\frac{\eta_r}{a_2\eta_u}\right)^{0.5} + C'_A(i)(T-A_f) \quad (7\text{-}4)$$

$$\eta = \eta_{ri}$$
$$C'_A(i)\left(\frac{\eta_{ri}}{a_2\,\eta_u}\right)^{0.5} + C'_A(i)(T-A_f) > \bar{\sigma} > C'_A(i)(T-A_f) \quad (7\text{-}5)$$

In the above equations, σ_s^{cr} and σ_f^{cr} are the phase transformation start and finish critical stresses which was material constants expressing the phase transformation behaviors of SMA. In order to describe the influences of phase transformation peak temperatures on the phase transformation behaviors of SMA, the phase transformation peak critical stress was introduced, and the expressions is given as follows:

$$\sigma_P^{cr} = \left(\sigma_f^{cr} - \sigma_s^{cr}\right)\frac{M_p - M_s}{M_f - M_s} + \sigma_s^{cr}$$

https://doi.org/10.1017/jmech.2012.56 Published online by Cambridge University Press

S_1, S_2, a_1 and a_2 are the material constants determined by the transformation peak temperature and peak critical stress, as follows:

$$S_1 = \frac{-1}{(\sigma_s^{cr} - \sigma_f^{cr})(\sigma_p^{cr} - \sigma_s^{cr})} \qquad S_2 = \frac{-1}{(\sigma_s^{cr} - \sigma_f^{cr})(\sigma_p^{cr} - \sigma_f^{cr})}$$

$$a_1 = \frac{-1}{(A_f - A_s)(A_p - A_s)} \qquad a_2 = \frac{-1}{(A_f - A_s)(A_p - A_f)}$$

$\bar{\sigma}$ is equivalent stress $\bar{\sigma} = \sqrt{\sigma'_{ij}\,\sigma'_{ij}/2}$ and σ'_{ij} is deviatoric stress tensor. It is easy to prove that $\bar{\sigma}=\sigma$ in one-dimensional state. η_u is the initial value of shape memory factor during the process of unloading. The evolution curve of shape memory residual factor with stress is shown in Fig. 5. One should note that in this work the shape memory residual factor is not accumulated with the number of cycles, which only describes the recover ability of material during one cycle. In the subsequent loading process, the value of shape memory factor still change from 0 to 1.

8. ONE-DIMENSIONAL MACROMECHANICAL CONSTITUTIVE EQUATION

In this section, we assume shape memory alloy to be an isotropic material, and based on the thermodynamic theory, a one-dimensional macromechanical constitutive equation is established by using the expression of Gibbs free energy. The total strain of SMA is divided into three parts: Elastic strain ε_e, shape memory strain ε_s and thermal expansion strain ε_T

$$\varepsilon = \varepsilon_e + \varepsilon_s + \varepsilon_T \tag{8}$$

According to the foregoing definition of shape memory factor and its physical meaning, the shape memory strain of SMA can be expressed as:

$$\varepsilon_s = \eta\varepsilon_L \tag{9}$$

The thermal expansion strain is expressed as

$$\varepsilon_T = \alpha(T - T_0) \tag{10}$$

where α is the thermal expansion coefficient which is independent upon the number of cycles.

From Hooke's law, the elastic strain can be expressed as follows

$$\varepsilon_e = \frac{\sigma}{E} \tag{11}$$

here E is the function of shape memory factor, expressed as [25]

$$E(\xi) = \left((1-\xi)E_A^{-1} + \xi E_M^{-1}\right)^{-1} \tag{12}$$

ξ is the martensite volume fraction.

Thus, the total strain of SMA can be express as follows

$$\varepsilon = \frac{\sigma}{E(\xi)} + \eta\varepsilon_L + \alpha(T - T_0)$$

Taking into account the residual strain, the total strain of shape memory alloy in the i^{th} cycle can be expressed as:

$$\varepsilon(i) = \frac{\sigma\left(E'_M(i)(1-\xi) + \xi E'_A(i)\right)}{E'_A(i)E'_M(i)} + \eta\varepsilon_L + \alpha(T - T_0) \tag{13}$$

In summary, the evolution equation of shape memory residual factor Eq. (2), elastic modulus Eq. (3), phase transformation critical stress Eq. (6) and the new phase transformation equation Eq. (7), compose the one-dimensional macromechanical constitutive equation. Comparing with previous models, the exponential relationship of critical stress, elastic modulus and cycle number is more reasonable. In addition, the solving process and parameter are clear contrasting to the generalized plasticity models. It can predict the thermomechanical behaviors of SMAs subjected to cyclic isothermal simple tension loading more precisely and comprehensively. Thus, it is easy to be used in practical applications.

9. THEORETICAL RESULTS AND DISCUSSIONS

In this section, the constitutive model is utilized to predict the hysteretic responses of superelastic SMA subjected to 20 cyclic isothermal simple tensions loadings by MATLAB software. In order to determine the material parameters of SMA, differential scanning colorimeter (DSC) tests and a series uniaxial tensile test were carried out at different temperatures, respectively. Based on the experimental results, the curves of critical stresses and temperature are plotted in Fig. 11. Therefore, phase transformation temperatures (A_s, A_f, M_s, M_f), material constants (S_1, S_2, a_1, a_2) and stress influence coefficients (C_M, C_A) can be obtained from the curves (as shown in Table. 1). It should be noted that, for simplicity, in this paper the elastic modulus of material after reverse transformation is assumed to be equal with that before martensite transformation.

Based on the material parameters obtained from the test results, the numerical results of SMAs subjected to uniaxial cyclic loading (i = 1, 8, 12, 18) are shown in Fig. 12. The dashed lines and red solid lines represent experimental results and numerical results, respectively. As can be seen from the curves of stress-strain, the value of residual strain in each loop gradually decreases with the increasing of cyclic-number. When i = 18, the value is close to 0, which indicates that the material gradually tends to be an approximately stable superelastic state.

https://doi.org/10.1017/jmech.2012.56 Published online by Cambridge University Press

Table 1 Material parameters used in numerical calculation

Phase transformation temperature	Material constant	Elastic modulus (i = 1)	Phase transformation Critical stress	Cycle-dependent parameters
A_s(^{0}C) = 16.58	S_1 = 7.31e-4	E_A(GPa) = 50	$\sigma^{cr}{}_s$ (MPa) = 281	B = 0.25
A_f(^{0}C) = 19.21	S_2 = –4.6e-4	E_M(GPa) = 34	$\sigma^{cr}{}_p$(MPa) = 304	ψ_1 =ψ_2 = 0.25
M_s(^{0}C) = 16.03	a_1 = –0.284	C_A = 7.0	$\sigma^{cr}{}_f$(MPa) = 340.4	$\overline{E}$ = 31GPa
M_f(^{0}C) = 12.18	a_2 = 0.295	C_M = 6.5	ε_L(%) = 8.3	a = 9.5e-6/K

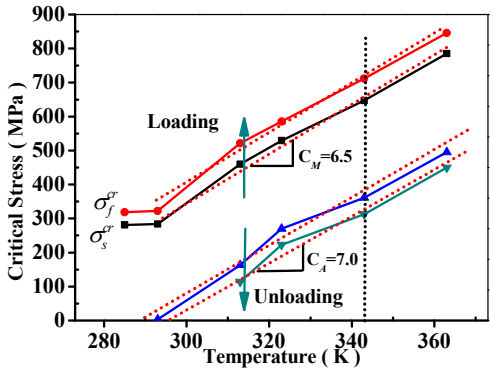
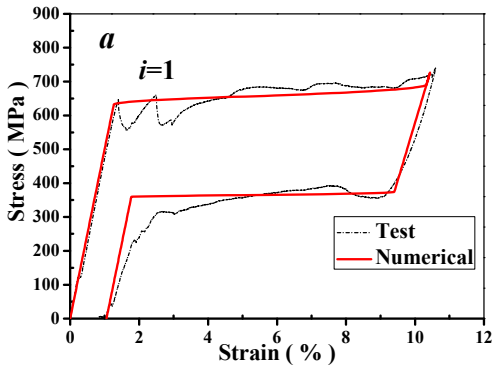
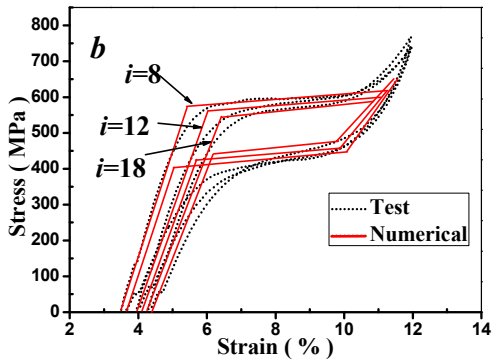


Fig. 11 The curves of critical stress and temperature (i = 1)



(a) i = 1



(b) i = 8, i = 12, i = 18

Fig. 12 Comparison of numerical results by proposed model and test results (343K, 3%/min)

During the process of cycle, the dissipated energy has an obviously decreasing tendency in the initial cycles (from i = 1to i = 8). However, the tendency becomes gentle in the following cycles (from i = 12 to i = 18). It can be seen from Fig. 12, the martensite critical stress gradually decreases and the austenite critical stress slightly increases with the number of cycles. The numerical results are in good agreement with experimental results, which validates the precision and rationality of constitutive model developed in present paper.

10. CONCLUSIONS

In this paper, based on the experimental results of uniaxial cyclic tensile of Ni-Ti SMA subjected to various strain-rates and temperatures, a macromechanical constitutive model was constructed to predict the cyclic mechanical behavior at constant temperature. In the proposed model, the residual strain is considered by introducing a new variable of shape memory residual factor and considering the effect of strain-rate and temperature. Then, simulations were carried out and compared with the experimental results based on the proposed model. The following conclusions were obtained:

1. A new variable of shape memory residual factor was introduced, which is related with the maximum shape memory strain. With the increasing of cycle numbers, the value of shape memory residual factor gradually approached to zero, and the materials would reach a stable state (nonlinear superelastic state). During the process of cyclic loading, the shape memory residual factor is not accumulated with the number of cycles. It only describes the recovery ability of material during one cycle.
2. Taking into account the influence of strain-rate and temperature, an exponential form equation was established to describe the evolution process of shape memory residual factor, elastic modulus and critical stress. Through the comparison between numerical results and test results, it's shown that the exponential form equation can well predict the evolution process.
3. Based on a series of uniaxial strain-controlled cyclic tensile tests of superelastic Ni-Ti SMA wires, a one-dimensional macromechanical constitutive equation was constructed taking into account the effect of cycle. The numerical results can demonstrate the validity of the present constitutive model to predict the cyclic mechanical behavior of SMA.

It should be noted that there are still some differences between our results and the results given in reference [12]. This may be the reason of the ignorance of the strain amplitude effect on residual strain in the present model.

ACKNOWLEDGEMENTS

This work is supported by the Fundamental Research Funds for the Central Universities (HEUCF20100201

https://doi.org/10.1017/jmech.2012.56 Published online by Cambridge University Press

and HEUCFZ1004), and the authors wish to acknowledge Harbin Engineering University of China.

REFERENCES

1. Brinson, L. C., "One-Dimensional Constitutive Behavior of Shape Memory Alloys: Thermomechanical Derivation with Non-Constant Material Functions and Redefined Martensite Internal Variable," *Journal of Intelligent Material Systems and Structures*, **4**, pp. 229–242 (1993).
2. Sun, Q. P. and Hwang, K. C., "Micromechanics Modeling for the Constitutive Behaviors of Polycrystalline Shape Memory Alloys," *Journal of Mechanics and Physics of Solids*, **41**, pp. 1–33 (1993).
3. Boyd, J. G. and Lagoudas, D. C., "A Thermodynamic Constitutive Model for the Shape Memory Materials Part II: The SMA Composite Material," *International Journal of Plasticity*, **12**, pp. 843–873 (1996).
4. Brocca, M., Brinson, L. C. and Bazant, Z. P., "Three-Dimension Constitutive Model for Shape Memory Alloys Based on Microplane Model," *Journal of Mechanics and Physics of Solids*, **50**, pp. 1051–1077 (2002).
5. Peng, X., Pi, W. and Fan, J., "A Microstructure-Based Constitutive Model for the Pseudoelastic Behavior of Niti SMAs," *International Journal of Plasticity*, **24**, pp. 966–990 (2008).
6. Zhou, B., Liu, Y. J., Leng, J. S. and Zou, G. P., "A Macro-Mechanical Constitutive Model of Shape Memory Alloys," *Science in China Series G: Physics, Mechanics & Astronomy*, **52**, pp. 1382–1391 (2009).
7. Feng, X. Q. and Sun, Q. P., "Shakedown Analysis of Shape Memory Alloy Structures," *International Journal of Plasticity*, **23**, pp. 183–206 (2007).
8. Lubliner, J. and Auricchio, F., "Generalized Plasticity and Shape Memory Alloys," *International Journal of Solids and Structures*, **33**, pp. 991–1003 (1996).
9. Gong, J. M., Tobushi, H., Takata, K. and Okumura, K., "Analysis and Simulation on Cyclic Superelastical Deformation Behavior of Tini Shape Memory Alloy Subjected to Loading And Unloading," *International Journal of Aeronautical Materialia*, **4**, pp. 6–12 (2002).
10. Mal´ecot, P., Lexcellent, C., Folt^ete, E. and Collet, M., "Shape Memory Alloys Cyclic Behavior: Experimental Study and Modeling," *International Journal of Engineering Materials Technology*, **l-28**, pp. 335–45 (2006).
11. Wael, Z. and Ziad, M., "A 3D Model of the Cyclic Thermomechanical Behavior of Shape Memory Alloys," *Journal of Mechanics and Physics of Solids*, **55**, pp. 2427–2454 (2007).
12. Saint-Sulpice, L., Chirani, S. A. and Calloch, S., "A 3D Super-Elastic Model for Shape Memory Alloys Taking Into Account Progressive Strain Under Cyclic Loadings," *Mechanical Materials*, **41**, pp. 12–26 (2009).
13. Auricchio, F., Reali, A. and Stefanelli, U., "A Three-Dimensional Model Describing Stress-Induced Solid Phase Transformation with Permanent Inelasticity," *International Journal of Plasticity*, **23**, pp. 207–226 (2007).
14. Kang, G. Z., Kan, Q. H., Qian, L. M. and Liu, Y. J., "Ratchetting Deformation of Superelastic and Shape Memory Niti Alloys," *Mechanical Materials*, **41**, pp. 139–153 (2009).
15. Kan, Q. H. and Kang, G. Z., "Constitutive Model for Uniaxial Transformation Ratchetting of Super-Elastic Niti Shape Memory Alloy at Room Temperature," *International Journal of Plasticity*, **26**, pp. 441–465 (2010).
16. Delville, R., Malard, B., Pilch, J., Sittner, P. and Schryvers. D., "Transmission Electron Microscopy Investigation of Dislocation Slip During Superelastic Cycling of Ni-Ti Wires," *International Journal of Plasticity*, **27**, pp. 282–297 (2011).
17. Ren, W. J., Li, H. N. and Song, G. B., "Phenomenological Modeling of the Cyclic Behavior of Superelastic Shape Memory Alloys," *Smart Materials and Structures*, **16**, pp. 1083–1089 (2007).
18. Lagoudas, D. C., Mayes, J. J. and Khan, M. M., "Simplified Shape Memory Alloy (SMA) Material Model for Vibration Isolation," *Proceedings of SPIE*, **4326**, pp. 452–461 (2001).
19. Tobushi, H., Shimeno, Y., Hachisuka, T. and Tanaka, K., "Influence of Strain Rate on Superelastic Properties of Tini Shape Memory Alloy," *Mechanical Materials*, **30**, pp. 141–150 (1998).
20. Nemat-Nasser, S. and Choi, J. Y., "Strain Rate Dependence of Deformation Mechanisms in a Ni–Ti–Cr Shape-Memory Alloy," *Acta Materialia*, **53**, pp. 449–454 (2005).
21. Nemat-Nasser, S. and Guo, W.-G., "Superelastic and Cyclic Response of Niti SMA at Various Strain Rates and Temperatures," *Mechanical Materials*, **38**, pp. 463–474 (2006).
22. Lee, W. S., Lin, C. F., Chen, T. H. and Hwang, H. H., "Effects of Strain Rate and Temperature on Mechanical Behaviour of Ti– 15Mo–5Zr–3Al Alloy," *Journal of Mechanical Biomedical Materials*, **1**, pp. 336–44 (2008).
23. Wang, Z. Q., Lei, H. S, Zhou, B. and Wang, Y. L., "Influence of Strain Rate on Mechanical Properties of Shape Memory Alloy," *Key Engineering Materials,* **467-469**, pp. 585–588 (2011).
24. Tanaka, K., "A Thermomechanical Sketch of Shape Memory Effects: One-Dimension Tensile Behavior," *Research Mechanical*, **18**, pp. 251–263 (1986).
25. Auricchio, F. and Sacco, E., "A One-Dimensional Model for Superelastic Shape Memory Alloys with Different Elastic Properties Between Austenite and Martensite," *International Journal of Non-linear Mechanical*, **32**, pp. 1101–1114 (1997).

(Manuscript received June 15, 2011,
accepted for publication January 9, 2012.)

https://doi.org/10.1017/jmech.2012.56 Published online by Cambridge University Press